

See discussions, stats, and author profiles for this publication at: <https://www.researchgate.net/publication/51122945>

# Comparative Model Studies of Gastric Toxicity of Nonsteroidal Anti-Inflammatory Drugs

ARTICLE *in* LANGMUIR · JUNE 2011

Impact Factor: 4.46 · DOI: 10.1021/la200499p · Source: PubMed

---

CITATIONS

9

READS

17

## 2 AUTHORS:



Michał Markiewicz  
Jagiellonian University  
15 PUBLICATIONS 49 CITATIONS

[SEE PROFILE](#)



Marta Pasenkiewicz-Gierula  
Jagiellonian University  
88 PUBLICATIONS 2,759 CITATIONS

[SEE PROFILE](#)

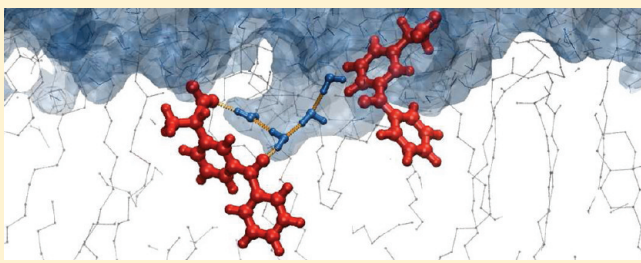
## Comparative Model Studies of Gastric Toxicity of Nonsteroidal Anti-Inflammatory Drugs

Michał Markiewicz and Marta Pasenkiewicz-Gierula\*

Department of Computational Biophysics and Bioinformatics, Faculty of Biochemistry, Biophysics and Biotechnology, Jagiellonian University, Kraków, Poland

 Supporting Information

**ABSTRACT:** A high percentage of people treated with a long-term nonsteroidal anti-inflammatory drug (NSAID) therapy suffer NSAID-induced gastrointestinal-tract-related side effects. A current hypothesis states that the side effects are related to the topical action of NSAID molecules on gastric mucus that lowers its resistance to luminal acid. The main lipids in human mucus are palmitoyloleoylphosphatidylcholine (POPC) and cholesterol (Chol). In this study, both X-ray diffraction and molecular dynamics (MD) simulation methods were employed to investigate the effects of selected NSAIDs in protonated and deprotonated states on the structural parameters of a POPC-Chol bilayer. The drugs were three commonly used NSAIDs with apparently different gastric toxicity: ketoprofen (KET), aspirin (ASP), and piroxicam (PXM). Both methods revealed that the effects of the NSAIDs on the POPC-Chol bilayer parameters were moderate and only slightly differentiated among the drugs. Much larger differences among the drugs were noticed in their interactions with interfacial water and  $\text{Na}^+$  as well as with the polar groups of POPC and Chol, mainly via H-bonds. Of the three NSAIDs, KET interacted with POPC and water the most extensively, whereas ASP interacted with Chol and  $\text{Na}^+$  more than did the other two. Interactions of PXM with POPC and Chol polar groups as well as with water and  $\text{Na}^+$  were limited.



### INTRODUCTION

Since the isolation of salicylic acid from willow bark and its first application as a drug to ease pain and reduce fever in 1828, pharmacologists' interest in nonsteroidal anti-inflammatory drugs (NSAIDs) has been steadily growing. NSAIDs are among the most commonly prescribed and used drugs in the world. Unfortunately, the widespread use of NSAIDs, among them aspirin, is connected with several adverse effects, mainly those related to the gastrointestinal tract such as ulcers and bleedings.<sup>1,2</sup> It is estimated that up to 30% of people treated with long-term NSAID therapy suffer NSAID-related side effects.<sup>3–6</sup> The etiology of the effects was first connected to NSAID-induced inhibition of prostaglandin synthesis,<sup>7–9</sup> which has a strong protective effect against gastric mucosal damage by luminal acid, bacteria, and their toxins.<sup>10</sup> However, another line of research showed that gastrointestinal tract injury and the inhibition of prostaglandin synthesis in the stomach mucosa are disconnected.<sup>11,12</sup> Therefore, an alternative hypothesis has been put forward that links NSAID-related side effects to their direct topical action on gastric mucus.<sup>12–14</sup> In a convincing experiment, it was shown that NSAIDs triggering gastric side effects affect the hydrophobicity of gastric mucosa, which increases its permeability and results in its lowered resistance to luminal acid<sup>15–17</sup> and possibly other factors. The gastric mucosa is protected against highly acidic environments by its outermost layer that constitutes an element of the hydrophobic barrier.<sup>16,18</sup> It is

believed that this layer is an oligolamellar structure made mainly of phospholipids.<sup>16,19</sup> NSAIDs, interacting with the phospholipids, decrease the hydrophobicity of the hydrophobic barrier.<sup>13,16,17,20</sup> This phospholipid–NSAID interaction was identified as a “chemical association”,<sup>14,21</sup> but its atomic-level details have not been elucidated so far. Nevertheless, the effect of NSAIDs on a phospholipid bilayer has been demonstrated. (See below.) It is possible that NSAIDs also affect physicochemical properties of the gastric mucosal cell membrane, which could add up to the harmful effect of NSAIDs on the acid-resistant barrier properties of mucosa.

To shed more light on the process of gastrointestinal tract injury by NSAIDs, a variety of biophysical methods have been applied to study the effects of NSAIDs on phospholipid aggregates, mainly bilayers (e.g., refs 12 and 21–24). The studies revealed that NSAIDs affect the thermotropic behavior of the bilayer<sup>12,22,24</sup> and suggested where the drug molecules are most likely located.<sup>23</sup> Moreover, NSAIDs significantly change lipid bilayer parameters such as the membrane thickness and fluidity, affect the mechanical properties, and lower the energy barrier for pore formation in the bilayer (ref 21 and references therein).

Received: July 4, 2010

Revised: April 18, 2011

Published: May 13, 2011

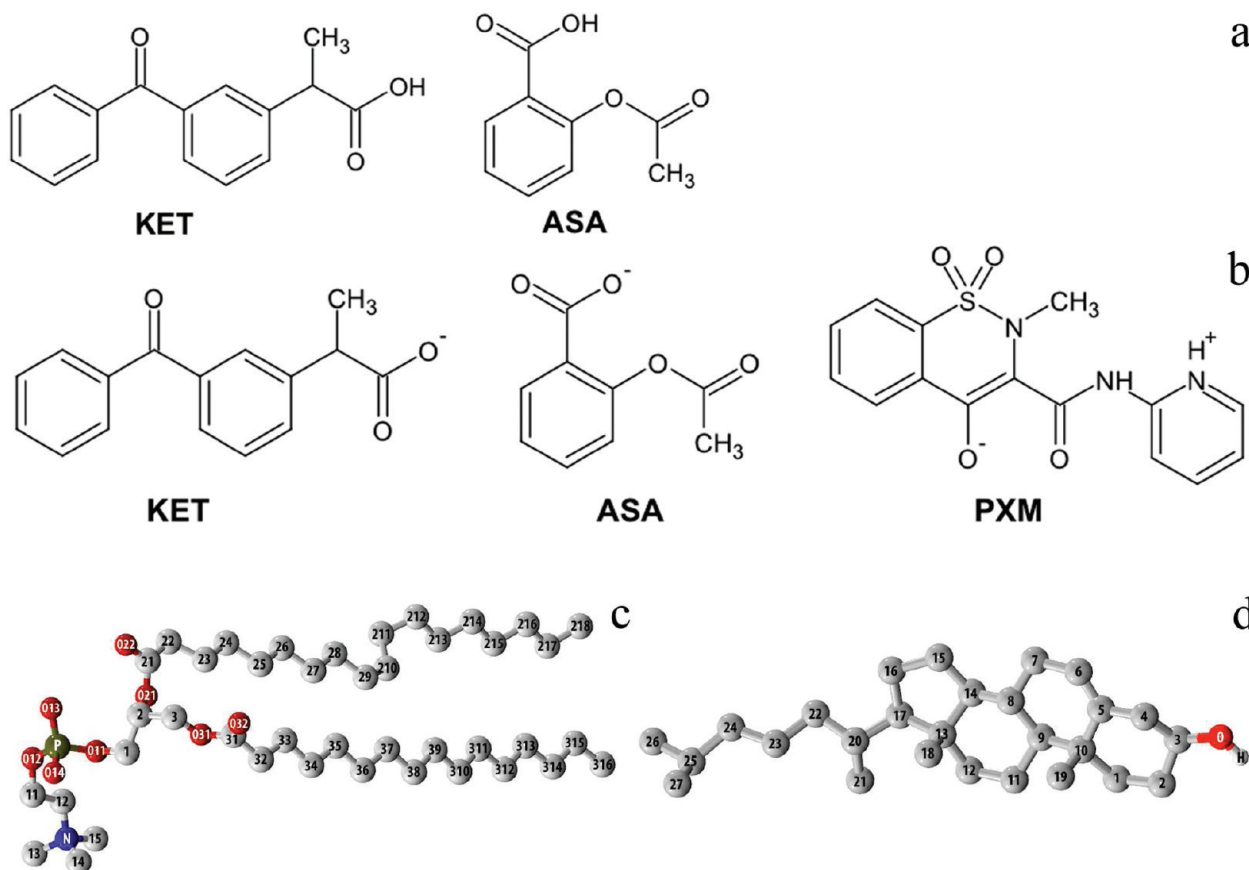


**Figure 1.** Chemical structures of (a) ketoprofen (KET) and aspirin (ASP) in their protonated neutral forms; (b) KET and ASP in their deprotonated anionic forms and piroxicam (PXM) in its zwitterionic form; (c) POPC with atom numbering; and (d) Chol with atom numbering. In c and d, gray represents carbon, red represents oxygen, and blue represents nitrogen atoms. The chemical symbol for carbon, C, is omitted.

Again, basic events that lead to changes in the properties of gastric mucosa induced by NSAIDs are still not known.

In the present study, an X-ray diffraction experiment and molecular dynamics (MD) simulations were applied to investigate the effects of three commonly used NSAIDs with apparently different gastric toxicities—ketoprofen (KET), aspirin (ASP), and piroxicam (PXM) (Figure 1a,b)—on the structure of a lipid bilayer and to describe the atomic-level interactions of the NSAIDs with lipids, water, and ions. The literature data concerning the gastric toxicity of the drugs used in this study are broadly distributed and contradict one another. According to the analysis of García-Rodríguez,<sup>25</sup> KET and PXM are very toxic and ASP is moderately toxic. Other sources offer results that PXM is more toxic than KET and ASP,<sup>26</sup> ASP is more toxic than PXM,<sup>20</sup> PXM is moderately toxic,<sup>27</sup> KET is very toxic, and ASP and PXM are weakly toxic.<sup>28</sup> However, the toxicity assigned to each drug depends on many factors and accepted criteria and may differ from study to study.<sup>26,27</sup>

The main phospholipid species found in human and pig mucus is phosphatidylcholine (PC) with one unsaturated hydrocarbon chain, mainly PC 16:0/18:1 (palmitoyloleoylPC, POPC, Figure 1c) and PC 18:0/18:2.<sup>29–31</sup> Also, cholesterol (Figure 1d) is present in rat,<sup>32</sup> bovine,<sup>33</sup> and human<sup>34,35,31</sup> gastric mucus. In aqueous solution, POPC molecules spontaneously form a bilayer into which cholesterol (Chol) intercalates easily. Biophysical studies indicate that a POPC-Chol bilayer constitutes a very hydrophobic barrier to polar and ionic species.<sup>36</sup> Thus,

one would expect that a bilayer is the predominant aggregation form of the phospholipids that make up the multilamellar hydrophobic layer protecting the gastric mucosa. For these reasons, in this study, we used a lipid bilayer composed of POPC and Chol as the most relevant lipid system. This bilayer played a double role: (1) as a model of a hydrophobic layer of phospholipids that protects gastric mucosa and (2) as a model of the gastric mucosa cell membrane.

Results of the X-ray diffraction measurements and MD simulations carried out in the present work give new details about the interactions of NSAIDs with membrane phospholipids, cholesterol, water, and ions, and they demonstrate a wealth of intermolecular contacts that differentiate the investigated drug molecules and their ionic states.

## MATERIALS AND METHODS

**X-ray Diffraction.** In the diffraction experiment, multilamellar liposomes of pure POPC (Figure 1c), POPC and Chol (Figure 1d), and POPC-Chol doped with drug molecules were used. POPC was purchased from Avanti Polar Lipids, and Chol and the drugs were purchased from Sigma-Aldrich. POPC; POPC and Chol in an ~7:2 molar ratio (22 mol % Chol); and POPC, Chol, and NSAIDs in a 7:2:1 molar ratio were mixed and dissolved in chloroform. The solvent was evaporated under nitrogen, followed by drying under a vacuum pump for 12 h. Redistilled water was added to each sample at lipid/H<sub>2</sub>O 1:10, 1:15, 1:25, and 1:30 molar ratios. The mixtures were centrifuged until

full homogenization occurred.<sup>37</sup> A few hours before the experiment, the samples were placed into sample holders. Small- (SAXS) and wide-angle X-ray scattering (WAXS) measurements were carried out at beamline A2 in HASYLAB at DESY using monochromatic X-ray radiation emitted by the DORIS synchrotron at a wavelength of 0.15 nm (fixed energy of 8 keV). SAXS and WAXS data collection was carried out with two linear position-sensitive gas-filled detectors. The SAXS detector was calibrated using rat-tail tendon, and the WAXS detector was calibrated using poly(ethylene terephthalate). The temperature and pressure were

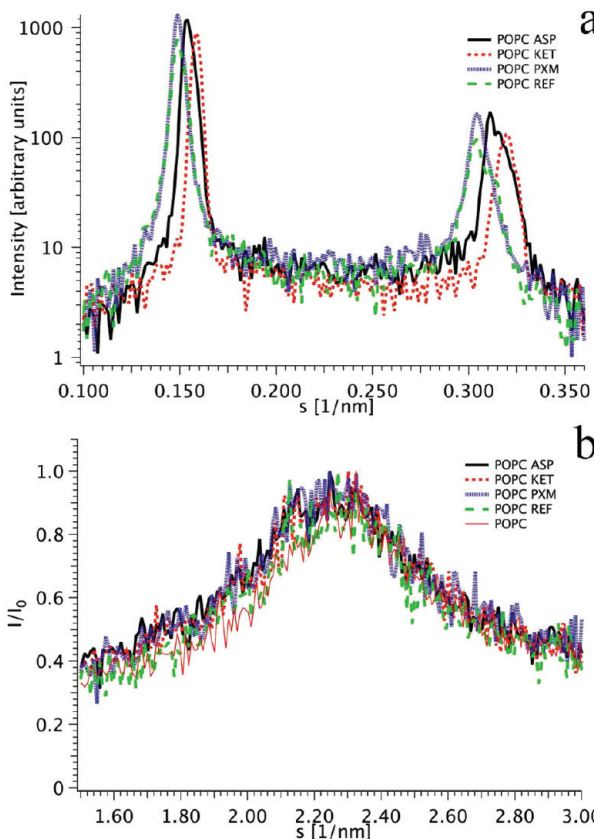


**Figure 2.** (a) Small-angle X-ray scattering (SAXS) profiles recorded for POPC-Chol and POPC-Chol-NSAIDs samples at 1:30 hydration and a temperature of 20 °C. (b) Wide-angle X-ray scattering (WAXS) profiles recorded for POPC, POPC-Chol, and POPC-Chol-NSAID samples at 1:30 hydration and a temperature of 20 °C.

**Table 1. Membrane Structural Parameters<sup>a</sup>**

bilayer	membrane width (Å)				average area per lipid (Å <sup>2</sup> )			
	X-ray		MD		X-ray		MD	
	$D_B$	$\Delta D_B$	$D_{HH}$	$\Delta D_{HH}$	A/PC	$\Delta A$	A/PC	$\Delta A$
POPC	35.9 ± 1.5		35.5 ± 0.1 <sup>b</sup>		70.0 ± 1.5		63.5 ± 0.5 <sup>b</sup>	
REF	38.3 ± 1.5	0	37.01 ± 0.07	0	65.5 ± 1.5	0	58.0 ± 0.5	0
KET	36.5 ± 1.5	-1.8 ± 2.1	36.74 ± 0.05	-0.27 ± 0.09	68.6 ± 1.5	3.1 ± 2.1	61.2 ± 0.7	3.2 ± 0.9
ASP	37.4 ± 1.5	-0.9 ± 2.1	36.89 ± 0.07	-0.12 ± 0.1	66.7 ± 1.5	1.2 ± 2.1	60.5 ± 0.9	2.5 ± 1.0
PXM	38.6 ± 1.5	0.3 ± 2.1	36.99 ± 0.04	-0.02 ± 0.08	65.1 ± 1.5	-0.4 ± 2.1	59.9 ± 0.6	1.9 ± 0.8

<sup>a</sup> The membrane width ( $D_B$ ,  $D_{HH}$ ) and average surface area per PC (A/PC) were obtained using an X-ray diffraction method (X-ray) and MD simulations (30–60 ns MD trajectory) for the studied bilayers. Errors in  $D_{HH}$  are standard error estimates, errors in A/PC for the simulated systems are standard deviation estimates, and errors in the experimental values  $D_B$  and A/PC are rough estimates. (See the text.)  $D_{HH}$ , distance between the maxima in the POPC P atoms' density profile across the bilayer;  $D_B$ , Luzzati bilayer width;  $\Delta D$ , difference between the width of the membrane containing NSAIDs and the reference system;  $\Delta A$ , difference between A/PC for the membrane containing NSAIDs and the reference system. <sup>b</sup> Reference 68.

controlled independently during the measurements. Positions of the lamellar peaks in the diffractogram (Figure 2a) were determined by nonlinear least-squares fitting to the Gaussian function. The bilayer width ( $D_B$ ) and subsequently the average cross-sectional area per lipid (A/PC) were estimated using the Luzzati method<sup>38</sup> and are given in Table 1.  $D_B$  is defined as the distance between the borders of two independent, nonmixing phases—water and lipid—and can be obtained from the real-space position of the first lamellar peak (and/or twice the position of the second peak) in the diffractogram for the bilayer at full hydration using the equation<sup>38</sup>

$$D_B = \frac{d(V_{PC} + nV_{Chol})}{V_{PC} + nV_{Chol} + mV_{H_2O}} \quad (1)$$

where  $d$  is the lattice parameter (lamellar repeat period,  $d = 1/s$ , where  $s$  is the position of the first peak in Figure 2a),  $n$  is the Chol/POPC molar ratio,  $m$  is the H<sub>2</sub>O/POPC molar ratio. The partial molecular volumes of POPC ( $V_{PC} = 1256 \text{ Å}^3$ <sup>39,40</sup>), Chol ( $V_{Chol} = 630 \text{ Å}^3$ <sup>39</sup>), and water ( $V_{H_2O} = 30 \text{ Å}^3$ <sup>41</sup>) were taken from the literature.

A/PC is related to  $D_B$  by the inverse proportion

$$A/PC = \frac{2V_{PC}}{D_B} \quad (2)$$

To avoid the artifacts connected with the lattice defects and to minimize the error in estimating the bilayer width at full hydration arising from the fact that some of the water occupies the interliposome space, the measurements were carried out at four hydrations (see above). SAXS and WAXS profiles for all measured samples at 1:30 hydration and a temperature of 20 °C are compared in Figure 2a,b, respectively. The samples were first measured at 20 °C and then heated to 40 °C and cooled to the starting temperature, and the recorded patterns were examined for the signs of lipid dehydration or phase transitions. The exemplary temperature scans (animation) for the POPC-Chol and POPC-PXM samples at various hydrations are attached as movie M1000 (Supporting Information). The scans do not show any phase transitions in the studied samples. The SAXS patterns (Figure 2a) and the broad WAXS peaks (Figure 2b) are typical of the liquid lamellar phase. The studied bilayers contained 22 mol % Chol. At this Chol content and these measurement temperatures, there are two coexisting phases in the bilayer: the liquid-disordered, Id, and liquid-ordered, lo. The lo phase might be responsible for a small shoulder in the second lamellar peak of the SAXS pattern for most samples (Figure 2a). The A/PC value of 70 Å<sup>2</sup> for the POPC bilayer at full hydration (Table 1) calculated from eqs 1 and 2 compares well to that of 68.2 Å<sup>2</sup> obtained by Kucerka et al.<sup>40</sup>

**MD Simulation.** *Simulation Systems.* The reference lipid bilayer used in this comparative MD simulation study consisted of 132 POPC and 36 Chol molecules (~22 mol % Chol) (POPC-Chol bilayer) and 5000 water molecules. To this bilayer, 16 NSAID molecules of each of the three chemical types were added in place of six POPC and two Chol molecules. Thus, three additional systems were created, each containing 126 POPC, 34 Chol, and 16 NSAID molecules. The pH of the stomach is in the range from below 1 to over 4.<sup>42</sup> The  $pK_a$  for ASP is 3.48,<sup>43</sup> for KET there are two literature  $pK_a$  values (3.98<sup>44</sup> and 4.6<sup>45</sup>), and the  $pK_a$  for the PXM OH group is 1.86 and that for the  $\text{NH}^+$  group is 5.46.<sup>46</sup> These  $pK_a$  values are within or slightly exceed the range of the stomach pH values except for the PXM  $\text{NH}^+$  group. In this study, we assumed that the pH of each simulation system corresponds to the  $pK_a$  of the NSAID in the bilayer (i.e., the situation where half of the NSAID molecules are in the neutral and half are in the deprotonated state). However, in the stomach pH range, the PXM  $\text{NH}^+$  group is protonated so PXM as well as POPC is in the zwitterionic form. Thus, each lipid bilayer contained 8 (50%) ASP or KET molecules in the neutral state and 8 in the anionic state or 16 PXM molecules in the zwitterionic state. The drug molecules had different initial conformations (see below).

Computer models of NSAID molecules were constructed using the Cerius2 program.<sup>47</sup> To create initial structures of the NSAIDs, the conformational search procedure was used. The minimum-energy conformers of each NSAID were generated by full rotation around all  $n$  flexible torsion angles (Figure 1) with a 30° step. The resulting 12<sup>n</sup> structures were optimized using the Dreiding force field<sup>48</sup> and Gasteiger–Marsili charges.<sup>49</sup> Finally, the generated conformers were cross-superimposed, and those with rmsd values greater than 1.5 Å were selected. This gave, for each NSAID (except PXM) in each ionic form, four low-energy and structurally different conformers representing relatively distant points in the conformational space. For PXM, eight conformers were selected because of its zwitterionic form. This conformational diversity in the initial structures had an additional direct, positive effect on the quality of the atomic charges on NSAIDs (see below).

For each NSAID, four conformationally diverse molecules in neutral and in anionic forms (for PXM, there were 8 zwitterionic conformers) were placed in each leaflet (16 in total) of the POPC-Chol bilayer membrane. To compensate for the negative charges on the drugs and to mimic the physiological NaCl concentration, 22  $\text{Na}^+$  and 14  $\text{Cl}^-$  ions were added to bilayers containing anionic KET and ASP and 22  $\text{Na}^+$  and 22  $\text{Cl}^-$  ions were added to the reference bilayer and that containing PXM. The number of ions added to each system corresponded to the effective concentration of NaCl in a POPC bilayer such as that of normal saline (0.15 M NaCl).<sup>50</sup> Because of the comparative character of this study, the numbers of PC, cholesterol, and water molecules in the systems containing NSAIDs were the same. In total, four systems were constructed: (1) the reference POPC-Chol with a POPC/Chol molar ratio of ~7:2 (POPC-REF) and three POPC-Chol bilayers containing (2) ketoprofen (POPC-KET), (3) aspirin (POPC-ASP), and (4) piroxicam (POPC-PXM), with a POPC/Chol/NSAID molar ratio of 7:2:1. Because there are no data on the preferential location of NSAIDs in phospholipid bilayers, in the initial systems the molecules were inserted without favoring any particular location (Figure 3). Half of them were placed in the hydrophobic bilayer core, parallel to the POPC chains, and half were placed in the water phase near the interface, parallel to the membrane surface. Each of the systems was MD simulated for a total time of 60 ns.

**Simulation Parameters.** For PC, Chol, NSAIDs, and ions, OPLS parameters<sup>51</sup> and for water, TIP3P parameters<sup>52</sup> were used. The united-atom approximation was applied to the CH,  $\text{CH}_2$ , and  $\text{CH}_3$  groups of POPC and Chol. The polar group of cholesterol and the whole NSAID molecule were treated in full atomic detail. The atomic charges of NSAIDs in neutral and anionic states were obtained using the restrained electrostatic potential (RESP) method.<sup>53</sup> Because the RESP charges

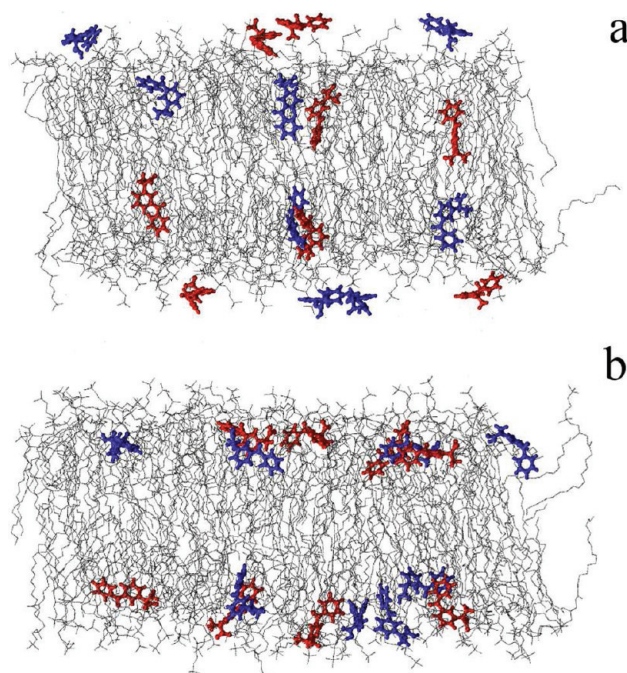


**Figure 3.** Example of the (a) initial locations of KET molecules within the POPC-Chol bilayer after energy minimization and (b) the final locations after 60 ns of the MD simulation. Neutral KET molecules are blue, and anions are red in the stick representation. POPC and Chol molecules are gray in the line representation; for clarity, the water is not shown.

show a strong conformational dependence, charges were calculated for sets of previously generated, structurally diverse conformers (see above). First, each NSAID conformer was Hartree–Fock optimized at the 6-31G\* level of theory, then four molecular electrostatic potential surfaces were calculated and atom-centered charges were fitted to those surfaces. Then, for each of the drugs in each ionic form, charges were averaged using Boltzmann weighing. All quantum-mechanical calculations were performed using the Gaussian 03 program.<sup>54</sup>

**Simulation Conditions.** The SHAKE algorithm was applied to CH, OH, and NH bonds of NSAID, Chol, and water, and the time step was set at 2 fs. Because all of the systems contained charged molecules and ions, the long-range electrostatic interactions were evaluated by means of the PME summation method with the  $\beta$ -spline interpolation order of 5 and a direct sum tolerance of  $10^{-6}$ .<sup>55</sup> For the real box, 3D periodic boundary conditions with the usual minimum image convention and a cutoff of 12 Å were used. The list of nonbonded pairs was updated every five steps. Simulations were carried out at a constant temperature of 310 K = 37 °C, which is above the main phase-transition temperature for a pure POPC bilayer (~5 °C),<sup>56</sup> and a constant pressure of 1 atm. Both the temperature and pressure were controlled by the Berendsen method.<sup>57</sup> The relaxation times for temperature and pressure were set at 0.4 and 0.6 ps, respectively. The applied pressure was controlled anisotropically, where each direction was treated independently and the trace of the pressure tensor was kept constant (1 atm).

**Averages and Errors.** Average values of parameters characterizing the MD-generated bilayers are time averages calculated from a 30 ns production trajectory sampled by 1 ps time steps. The instantaneous (recorded every 1 ps) average cross-sectional area per POPC in the POPC-Chol bilayer and those containing drug molecules at a given time step was calculated in two steps: (1) From the total surface area of the bilayer, the area occupied by the Chol molecules of  $17(18) \times 39 \text{ Å}^2 = 663(702) \text{ Å}^2$  was subtracted; 17(18) is the number of Chol molecules in

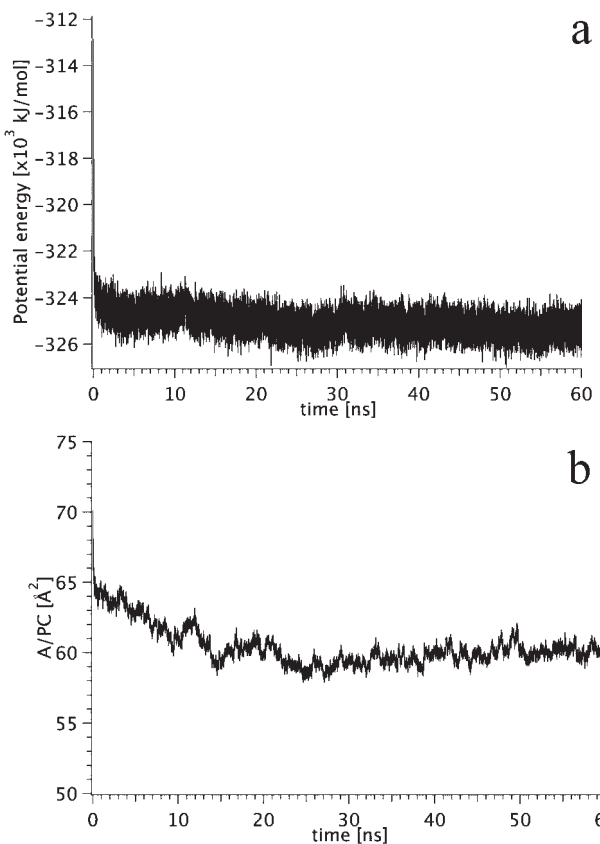


**Figure 4.** Time profiles of the (a) potential energy and (b) average surface area per POPC for the POPC-PXM bilayer.

one bilayer leaflet, and  $39 \text{ \AA}^2$  is the approximate average surface area of a Chol molecule obtained in the Chol monolayer studies<sup>58–60</sup> as well as in the Chol crystal.<sup>61</sup> (2) The resulting area was divided by the number of POPC molecules in one bilayer leaflet of 63(66). (The numbers in parentheses are for the POPC-REF bilayer.) For most average values, the associated errors are standard deviation estimates that provide information about the distributions of the data values. In the case of  $D_{\text{HH}}$  and  $S_{\text{mol}}$ , the errors in the average values, that is, the standard errors, were calculated over 5 blocks, with each being a 6 ns fragment of the productive trajectory. Errors in experimental values of  $D_B$  and  $A/\text{PC}$  (Table 1) were only approximately assessed on the basis of error estimates of the partial molecular volumes of POPC, Chol, and water.<sup>39</sup>

## RESULTS

**Membrane Systems Generated in MD Simulations—Equilibration.** Time profiles of the potential energy,  $E_{\text{POT}}$ , and the instantaneous average surface area per PC (see above) were recorded from the onset of simulation until 60 ns for each bilayer system. Examples of the profiles for the POPC-PXM bilayer are shown in Figure 4a,b, respectively. For the other bilayers, the profiles are in Figure S1 (Supporting Information). The average values of the potential energy and total simulation box area for equilibrated systems are in Table S1 (Supporting Information). On the basis of the time profiles, it was concluded that all four systems equilibrated thermally during the first 15 ns of MD simulations. However, a longer time was required for the drug molecules to settle at their equilibrium depth in the bilayer. Thus, a key initial step in the analyses below was to monitor their

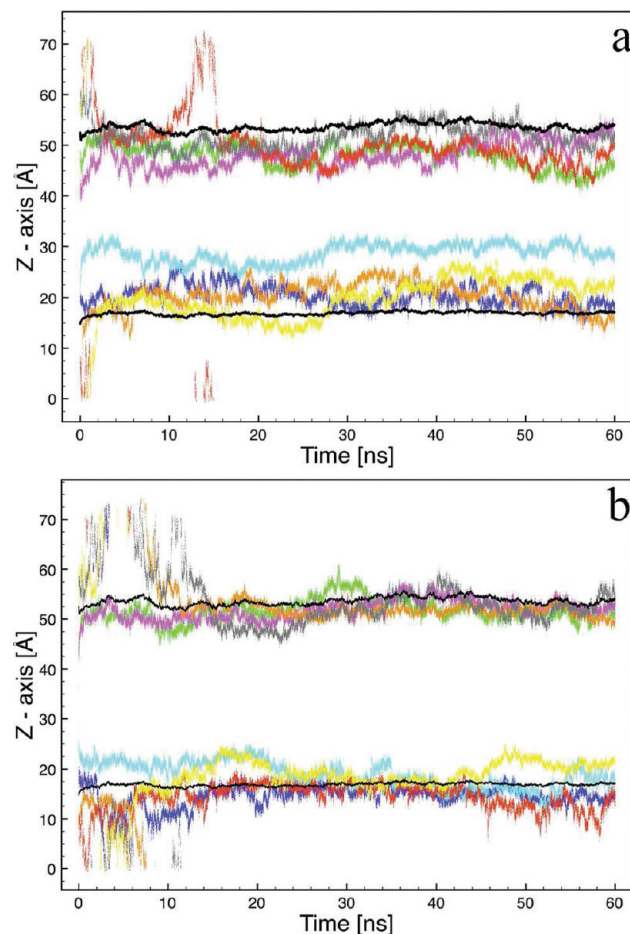


**Figure 5.** Time profiles of the location of the center of mass of (a) neutral and (b) negatively charged ASP molecules along the bilayer normal ( $z$  axis). Black lines indicate the average vertical location of P atoms in each of the bilayer leaflets. The periodic boundary conditions allow the translocation of drug molecules through the water phase between the two water layers.

vertical location in the bilayer as a function of time. Only after this location stabilized was it justified to carry out analyses.

Time profiles of the  $z$  coordinate of the center of mass (CM) of each NSAID molecule in the bilayer were recorded over the total simulation time of 60 ns. The profiles for the neutral and negatively charged ASP molecules in the bilayer are presented in Figure 5 and for KET and PXM in Figure S2 (Supporting Information). As the time of the NSAID locational equilibration varied from 10 ns for the neutral KET to 30 ns for PXM, because of the comparative character of the study, the first 30 ns of each simulation was not included in further analyses. The time profiles in Figures 5 and S2 indicate that after reaching their preferential depth in the bilayer the drug molecules do not change it radically during the observation time of 30 ns and are located in the vicinity of the bilayer interfacial region, with most of them on the hydrophobic core side. Atom mass density profiles across the bilayer for the atoms of the neutral and anionic drug molecules are shown in Figures 6 and S3 (Supporting Information). The profile of the anionic ASP atoms overlaps with that of the P atoms (Figure 6b), whereas that of the neutral ASP atoms is significantly shifted toward the bilayer center and is broad (Figures 6a and S3). Density distributions of the anionic and neutral KET atoms

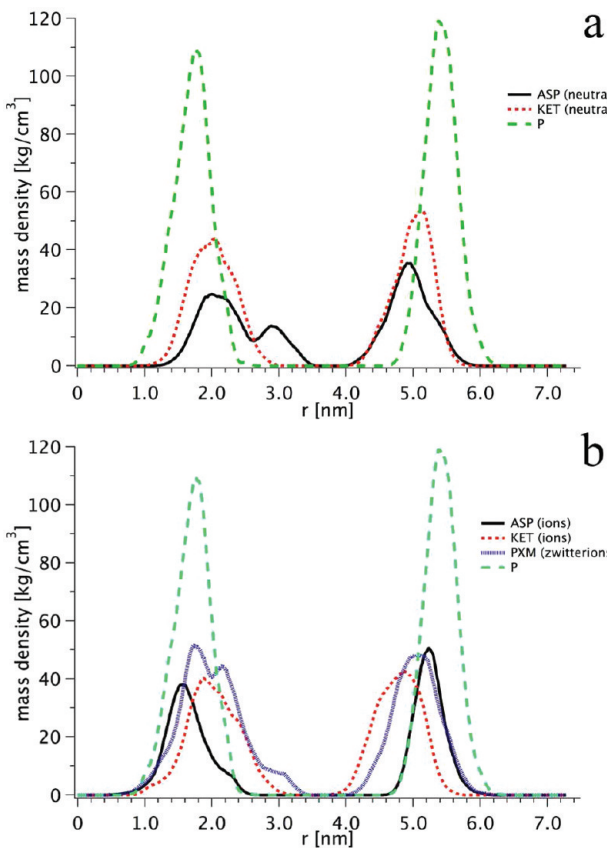


**Figure 6.** Mass density profiles along the bilayer normal ( $z$  axis) of the atoms of (a) neutral ASP and KET and (b) anionic ASP and KET and zwitterionic PXM in the respective bilayers relative to the density profile of the POPC P atoms in the POPC-ASP bilayer.

are moderately narrow and to a large extent overlap each other; however, they both are shifted toward the bilayer center relative to the distribution of the P atoms (Figures 6 and S3), and that for the anionic KET is even more shifted (Figure S3). The density profile of the PXM atoms is similar to that of the neutral ASP atoms. Although some of the drug molecules are located relatively deeply in the bilayer core, none of them diffused into the central region of the lowest density or translocated to the other leaflet of the bilayer (Figures 5 and S2).

**Effects of NSAIDs on the Bilayer. Spatial Properties of the Membrane.** The important structural parameters of a lipid bilayer are the average cross-sectional area per lipid,  $A/PC$ , and the bilayer width.  $A/PC$  and the width belong to a small group of membrane parameters that can be obtained by both the X-ray diffraction method and MD simulation. In the presented X-ray diffraction measurements, the bilayer width,  $D_B$ , was obtained using the Luzzati method and calculated from eq 1;<sup>38</sup> subsequently,  $A/PC$  was calculated from  $D_B$  using eq 2. However, the value of  $A/PC$  calculated from eq 2 is only approximate and is systematically too large.

The bilayer width and  $A/PC$  can be assessed independently of each other from the generated MD trajectories. The bilayer width has no exact definition, so here its value is estimated as the distance between the maxima in the POPC P atoms' density profile across the bilayer,  $D_{HH}$  (Figures 6 and S3, Supporting Information). The value of  $D_{HH}$  approximates the measure of the bilayer width as a head–head separation that can, in principle, be

obtained as the distance between the maxima in the experimental electron density profile. However, this is possible only when four<sup>62</sup> or, applying some mathematical methods, three orders of diffraction<sup>63</sup> are available. In the present study, only a two-peak diffraction pattern was recorded, so it was not possible to get  $D_{HH}$  from the experimental data. An extensive discussion of the relationship between  $D_B$  and  $D_{HH}$  is present in ref 62, and graphical representations of the relationship are in Figure 2 of ref 62 and Figure 2 of ref 63.

In this study, we are interested in the effect of NSAIDs on the membrane parameters rather than their exact values. Thus, in further analyses, changes in the parameter values caused by the presence of drug molecules in the bilayer relative to the values for the reference system (POPC-REF),  $\Delta A$  and  $\Delta D$ , were compared and their trends were monitored. The values of  $A/PC$ , the bilayer width,  $\Delta A$ , and  $\Delta D$  obtained from X-ray diffraction and MD simulation for all bilayer systems are presented in Table 1. A comparison of the entries in Table 1 indicates that the changes in  $A/PC$  and  $D_B$  obtained from experiment have the same trend as changes in  $A/PC$  and  $D_{HH}$  obtained from computer simulation.

**Chain Order.** The orientational arrangement of acyl chains in the membrane was evaluated using molecular order parameter  $S_{mol}$ .  $S_{mol}$  for the  $n$ th segment of an acyl chain is defined through<sup>64</sup>

$$S_{mol} = 0.5 \times \langle 3 \cos^2 \theta_n - 1 \rangle \quad (3)$$

where  $\theta_n$  is the instantaneous angle between the  $n$ th segmental vector (i.e., the  $(C_{n-1}, C_{n+1})$  vector linking  $n-1$  and  $n+1$  carbon (C) atoms in the acyl chain) and the bilayer normal and  $\langle \dots \rangle$  denotes both the ensemble and the time average.  $S_{mol}$  profiles along the  $\beta$  and  $\gamma$  chains averaged over both bilayer leaflets are, for the simulated bilayers, shown in Figure 7a and b, respectively.

The  $S_{mol}$  profiles are similar for all simulated systems; nevertheless, they indicate that the PC chains in the POPC-PXM bilayer are more ordered than in the POPC-REF bilayer.

**Interactions of NSAID with Water, POPC, and Cholesterol.** The following geometric criteria of a hydrogen bond (H-bond) were used in the analyses below: the distance between the H-bond donor (D) and the acceptor (A) is  $\leq 3.5$  Å, and the angle between the A–D vector and the D–H bond is  $\leq 30^\circ$ .

**NSAID–Water Hydrogen Bonds.** Radial distribution functions (RDF) of the oxygen atoms in water and the NSAIDs in the neutral (Figure 8a) and anionic (Figure 8b) states (O–O RDF) were calculated to examine whether NSAID molecules embedded in the bilayer do interact with water. The RDFs in Figure 8a show that neutral ASP and KET and zwitterionic PXM make H-bonds with water to a similar but moderate extent, whereas the H-bonding of anionic ASP and KET with water is significantly more extensive (Figure 8b). To understand better the observed differences in the extent of H-bonding, RDFs of the water oxygen atoms were calculated relative to each oxygen atom of the NSAIDs in the neutral and anionic states (Figure 9). Because PXM has, in addition to oxygen atoms, nitrogen atoms, PXM(N)-WAT(O) RDFs were also calculated (Figure 9f). The average numbers of NSAID···water H-bonds per NSAID for each of the studied drugs were calculated directly on the basis of the geometric criteria (above) and are given in Table 2. Figure 9a–d shows that in these interactions the acceptors of H-bonds are the oxygen atoms of the carboxylic and carbonyl groups of both neutral and ionic KET and ASP and all of the oxygen atoms of zwitterionic PXM but none of the nitrogen

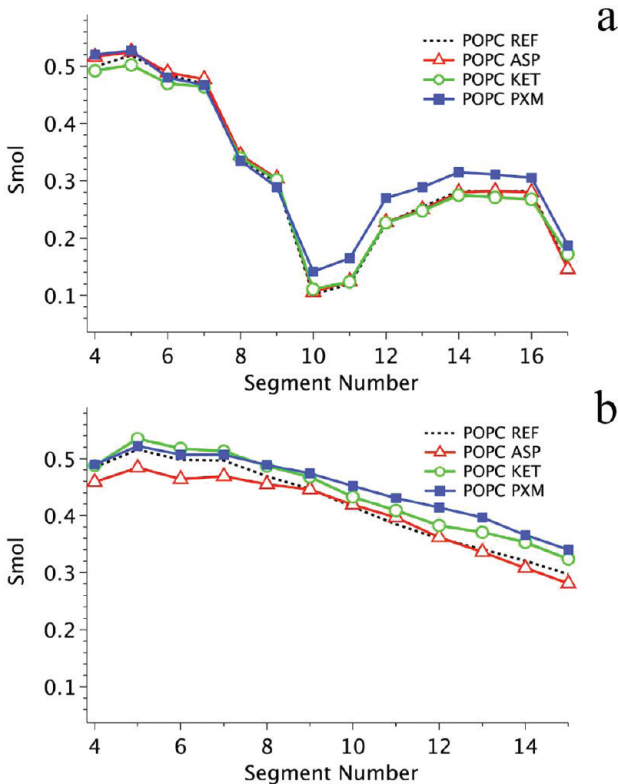


**Figure 7.** Molecular order parameter ( $S_{\text{mol}}$ ) profiles calculated for the POPC (a)  $\beta$  chain and (b)  $\gamma$  chain for the bilayers containing KET, ASP, and PXM as well as the reference system (POPC-REF). The standard errors, on the order of 0.01, are less than the size of the symbols.

atoms (Figure 9e,f). By far, the largest numbers of H-bonds with water make oxygen atoms of the ionized KET carboxylic group (Figure 9c). The average numbers of H-bonds of water with the POPC nonesterified phosphate oxygen atoms (Figure 1c), collectively called as Op, and carbonyl oxygen atoms (Figure 1c), collectively called as Oc, per POPC are given in Table 3 (last column); they indicate that NSAIDs practically do not affect the binding of water by POPC.

The dynamics of H-bonds between the water molecules and the NSAID oxygen atoms in the bilayer was analyzed using the hydrogen bond time correlation function,  $C_{\text{HB}}$ ,<sup>65</sup> defined as

$$C_{\text{HB}}(\tau) = \frac{\langle h_{Nw}(t_0) h_{Nw}(t_0 + \tau) \rangle}{\langle h_{Nw} \rangle} \quad (4)$$

where  $h_{Nw}(t)$  is a binary function of unity when a particular water molecule and a particular NSAID oxygen atom are H-bonded at time  $t$  and zero otherwise.  $\langle \dots \rangle$  denotes averaging over all considered NSAID $\cdots$ water H-bonds and over initial time values  $t_0$ . Physically,  $C_{\text{HB}}$  represents the probability that the bond existing at  $t = t_0$  still exists after a delay of  $\tau$  and allows for temporal breaks. The average lifetimes of NSAID $\cdots$ water H-bonds estimated by integrating the  $C_{\text{HB}}$  functions are given in Table 2.

**NSAID-POPC Hydrogen Bonds.** Calculated NSAID-PC O–O and N–O RDFs (Figure 10) clearly show that ASP and KET make H-bonds with POPC. Because PC is only an H-bond acceptor, NSAID $\cdots$ PC can be formed merely with NSAIDs in the neutral or zwitterionic form. In these interactions, the H-bond donor is the COOH group of ASP and KET. In the case of PXM,

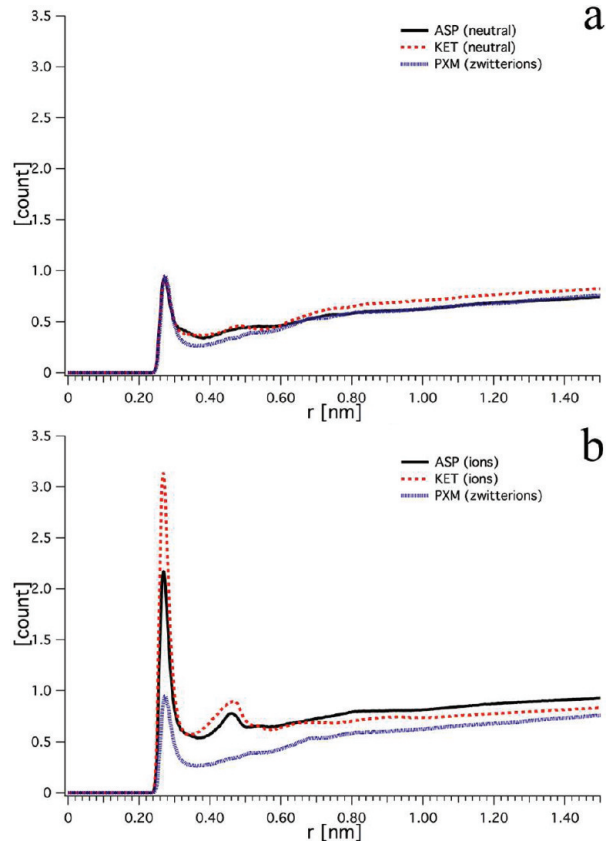


**Figure 8.** NSAID–water radial distribution functions of the water oxygen atoms relative to all oxygen and nitrogen (in the case of PXM) atoms of the NSAID molecule in the (a) neutral and (b) anionic as well as zwitterionic forms.

the H-bond donor could be the amine group and/or pyridinium, but neither makes H-bonds with POPC (Figure 10a). The H-bond acceptors are the POPC Op atoms. The average numbers of NSAID $\cdots$ POPC H-bonds are given in Table 4.

Because the number of NSAID $\cdots$ POPC H-bonds is small (Table 4), it was improper to use eq 4 to evaluate their lifetimes. Instead, binding and nonbinding states between a particular NSAID molecule of a given type and a particular oxygen atom of the POPC molecule were directly recorded. An example of the binding time profile for arbitrarily chosen KET $\cdots$ POPC is shown in Figure 11a, where 1 indicates binding, 0 indicates nonbinding, and the vertical lines indicate transitions between binding and nonbinding states. The profiles were calculated for each NSAID molecule, and from these time profiles, the NSAID $\cdots$ POPC H-bonding lifetimes were estimated as an average over eight neutral ASP and KET molecules because PXM does not make H-bonds with POPC (Figure 10a). When calculating the lifetime, only binding events longer than 20 ps were taken into account and breaks shorter than 150 ps were ignored. The 20 and 150 ps thresholds were chosen on the basis of distributions of the firm binding (Figure 11b) and break times. The number of NSAID $\cdots$ POPC H-bonds and their estimated lifetimes are given in Table 4. These calculations are, however, very approximate, and the errors in the derived values are large (Table 4 and Figure 11).

**NSAID-POPC Charge Pairs.** Electrostatic interactions between charged groups of NSAIDs ( $O^-$  of an ionized hydroxyl group

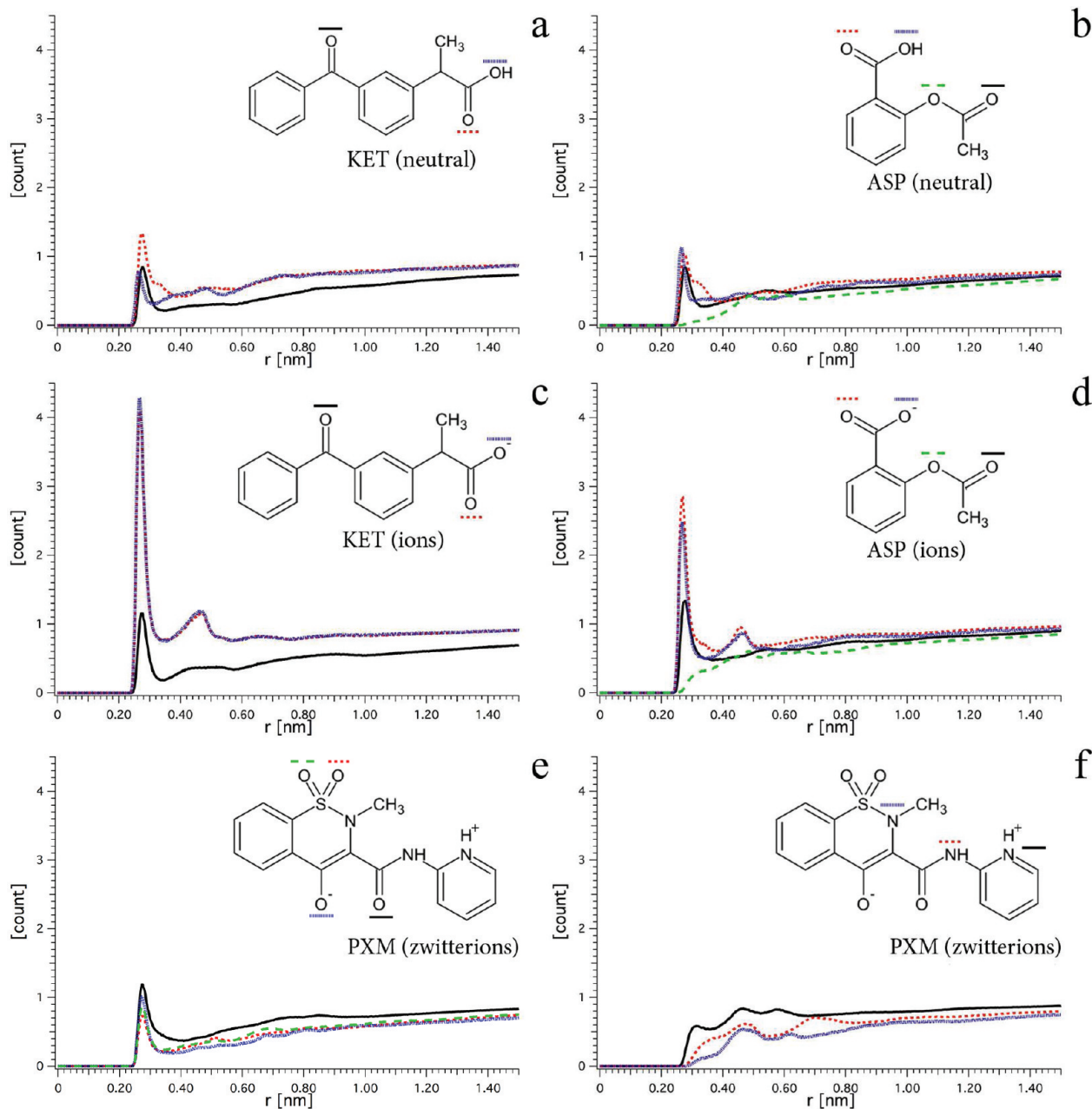


**Figure 9.** (a–e) NSAID–water radial distribution functions (O–O RDF) of the water oxygen atoms relative to each oxygen atom of the NSAID molecules in the neutral (a) KET and (b) ASP, anionic (c) KET and (d) ASP, and zwitterionic (e) PXM, states. (f) N–O RDF of the water oxygen atoms relative to each nitrogen atom of PXM.

**Table 2. Hydrogen Bonds of NSAIDs with Water<sup>a</sup>**

bilayer	HB/NSAID	HB lifetime (ps)
KET – neutral/anions	1.31 ± 0.29/4.63 ± 0.49	159/135
ASP – neutral/anions	1.10 ± 0.26/3.28 ± 0.49	56/148
PXM – zwitterions	1.94 ± 0.25	208

<sup>a</sup> Average numbers of NSAID···water H-bonds per NSAID molecule (HB/NSAID) and the estimated lifetimes of the H-bonds in the bilayers containing NSAIDs. Errors in HB/NSAID are standard deviations.

and NH<sup>+</sup> of pyridinium) and POPC (a positively charged choline group and negatively charged Op atoms) were examined by calculating the relevant RDFs (Figure 10b). The RDFs

**Table 3. Binding of Na<sup>+</sup> by NSAIDs and POPC<sup>a</sup>**

bilayer	%Na <sup>+</sup>			
	NSAID	%Na <sup>+</sup> Op	%Na <sup>+</sup> Oc	HB/POPC
KET	19 ± 5	85 ± 10	50 ± 7	4.3 ± 0.1
ASP	30 ± 5	80 ± 6	49 ± 5	4.4 ± 0.1
PXM	8 ± 4	80 ± 7	57 ± 9	4.1 ± 0.1
REF	79 ± 5	52 ± 5	4.3 ± 0.1	

<sup>a</sup> Percentage of Na<sup>+</sup> bound to KET, ASP, and PXM in the respective bilayers as well as to POPC Op and Oc atoms in the studied bilayers. Each bilayer contains 22 Na<sup>+</sup> ions. Average number of water H-bonds with the POPC Op and Oc atoms per POPC (HB/POPC). Errors are standard deviations.

demonstrate that such interactions take place but are not numerous.

**NSAID-Chol Hydrogen Bonds.** Because Chol can act as both an H-bond acceptor and donor, NSAID $\cdots$ Chol can be formed with NSAIDs in neutral, zwitterionic, and anionic forms. Calculated NSAID-Chol O–O and N–O RDFs (Figure 12) clearly show that ASP, KET, and PXM form H-bonds with Chol, however only in the ionic or zwitterionic form. In these interactions, none of the potential NSAID's H-bond donor group participates in the NSAID $\cdots$ Chol H-bonds. The exclusive H-bond donor is the Chol hydroxyl group, and the acceptors are the oxygen atoms of the ionized NSAID carboxylic groups except for PXM, where the H-bond acceptors are the sulfonyl oxygen atoms (cf. Figure 1). The average numbers and lifetimes

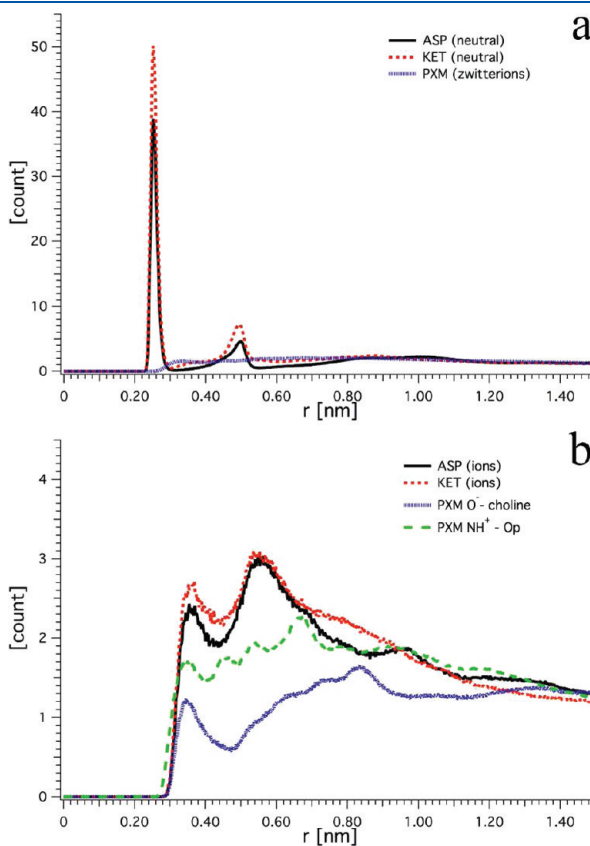


**Figure 10.** (a) NSAID-POPC radial distribution functions of the POPC phosphate oxygen atoms relative to the OH (O–O RDF) and NH (N–O RDF) groups of ASP, KET, and PXM. (b) RDF of the ASP, KET, and PXM O– and CH<sub>3</sub> groups of the positively charged choline moiety of POPC (O–choline<sup>+</sup> RDF) and of the NH<sup>+</sup> of pyridinium and the negatively charged phosphate oxygen atoms of POPC (N<sup>+</sup>–O– RDF).

**Table 4. Hydrogen Bonds of NSAID with POPC and Chol<sup>a</sup>**

bilayer	NSAID $\cdots$ POPC		NSAID $\cdots$ Chol	
	HB/NSAID	HB lifetime (ps)	HB/NSAID	HB lifetime (ps)
KET – neutral/anions	0.70 $\pm$ 0.14	669.46	0.0/0.06 $\pm$ 0.06	25/190.69
ASP – neutral/anions	0.53 $\pm$ 0.10	1149.6	0.0/0.27 $\pm$ 0.06	56.15/597.55
PXM – zwitterions	0.0	0.0	0.06 $\pm$ 0.03	152.77

<sup>a</sup> Average numbers of the neutral NSAID $\cdots$ POPC and NSAID $\cdots$ Chol H-bonds per NSAID molecule (HB/NSAID) and their estimated lifetimes in the bilayers containing NSAIDs. Errors in the lifetime values are on the order of 2000 ps.

of NSAID $\cdots$ Chol H-bonds derived under the same criteria as in the case of NSAID $\cdots$ POPC H-bonds are presented in Table 4. ASP makes significantly more H-bonds with Chol than do KET and PXM.

**Interactions of NSAID, POPC, and Cholesterol with Ions.** Atom mass density profiles showing the distributions of water O, POPC P, Chol O, and NSAID atoms and Na<sup>+</sup> and Cl<sup>–</sup> along the bilayer normal in the reference and containing NSAID bilayers are shown in Figure S3 (Supporting Information).

**NSAID–Ion Interactions.** RDFs of Na<sup>+</sup> relative to oxygen atoms of ASP and KET in the neutral (Figure 13a) and anionic (Figure 13b) forms as well as of Na<sup>+</sup> and Cl<sup>–</sup> relative to oxygen and nitrogen atoms of zwitterionic PXM (Figure 13b) were calculated to examine whether NSAID–ion interactions take place in the bilayers. The RDFs in Figure 13 show that neutral ASP does not interact with Na<sup>+</sup>; neutral KET and zwitterionic

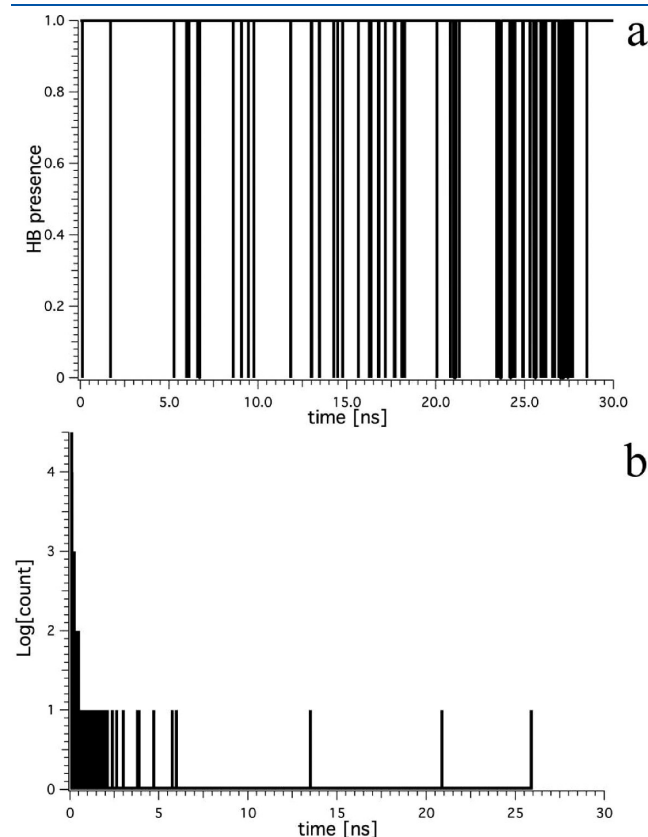


**Figure 11.** (a) Time profile of binding for an arbitrarily chosen KET $\cdots$ POPC H-bond (after equilibration). 1 indicates binding, 0 indicates nonbinding, and the vertical lines indicate transitions between binding and nonbinding states. (b) Distributions of firm binding times of the KET $\cdots$ POPC H-bonds.

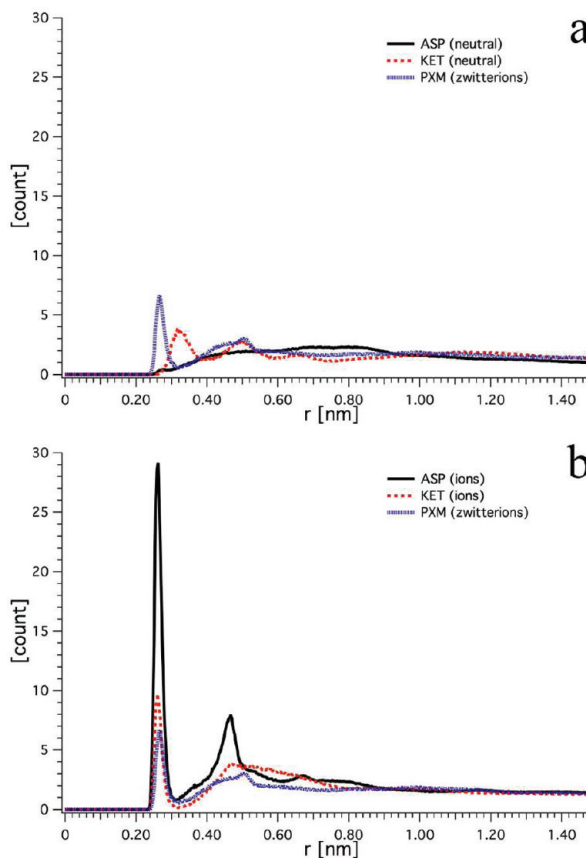


**Figure 12.** NSAID-Chol radial distribution functions (O–O RDF) of the Chol oxygen atoms relative to oxygen atoms of NSAIDs in the (a) neutral and (b) anionic as well as zwitterionic states.

PXM interact with  $\text{Na}^+$  weakly, but PXM (as well as ASP and KET) does not interact with  $\text{Cl}^-$ . Of the two anionic NSAIDs, ASP interacts with  $\text{Na}^+$  more extensively than does KET. To identify the  $\text{Na}^+$  binding sites of ASP, KET, and PXM, RDFs of  $\text{Na}^+$  were calculated relative to each oxygen atom in the NSAIDs (Figure S4, Supporting Information). Figure S4 shows that  $\text{Na}^+$  interacts predominantly with both oxygen atoms of the ionized carboxylic groups of ASP and KET and the oxygen atoms of the ionized hydroxyl and the carbonyl groups of PXM. Of the 22  $\text{Na}^+$  ions in each bilayer, 30% are bound by ASP, 19.5% are bound by KET, and 8% are bound by PXM. In most cases, one  $\text{Na}^+$  is simultaneously bound by two oxygen atoms of NSAID molecules and in the case of ASP even by four oxygen atoms. In effect, the ratio of the number of interactions between NSAID oxygen atoms and  $\text{Na}^+$  in the ASP-, KET-, and PXM-containing bilayers is roughly 1: $\frac{1}{2}$ : $\frac{1}{4}$ ; the ratio is reflected in the RDFs in Figure S4 (Supporting Information). To discriminate between the bound and nonbound ions, the distance criterion was used, where the limiting interaction distance corresponded to the first minimum in the NSAID- $\text{Na}^+$  RDF of 3 Å. The percentage of NSAID-bound ions in each bilayer is given in Table 3.

**POPC–Ion and Chol–Ion Interactions.** The RDFs of  $\text{Na}^+$  relative to Op and Oc of POPC are very similar for the three bilayers containing NSAIDs as well as for the reference bilayer (Figure S5, Supporting Information). The percentages of the Op- and Oc-bound ions in the reference and drug-containing bilayers are given in Table 3. The drug molecules practically do

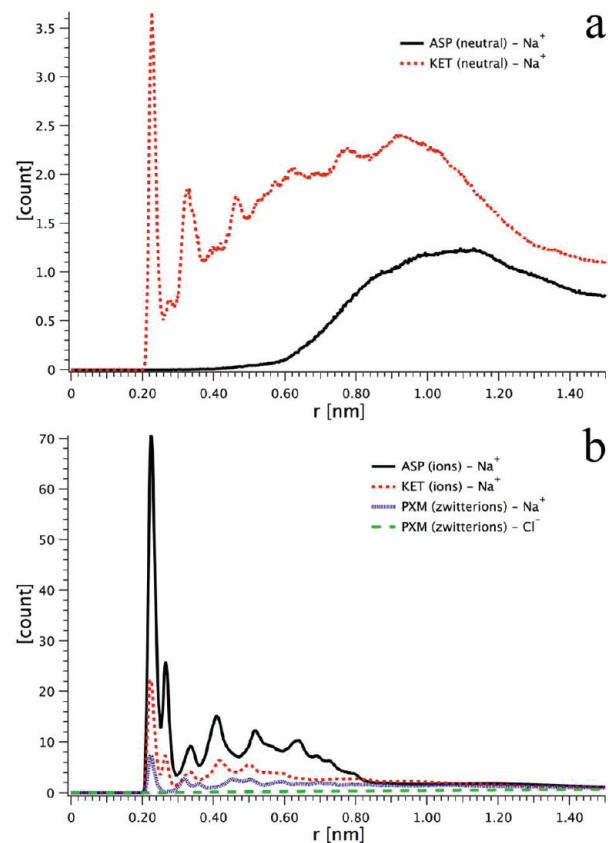


**Figure 13.** NSAID–ion radial distribution functions of (a)  $\text{Na}^+$  relative to oxygen atoms of ASP and KET in the neutral state and (b)  $\text{Na}^+$  relative to oxygen atoms of anionic ASP and KET and zwitterionic PXM as well as  $\text{Cl}^-$  relative to the pyridinium nitrogen atoms of PXM.

not affect the binding of  $\text{Na}^+$  by POPC. Cholesterol essentially does not bind  $\text{Na}^+$ .

## DISCUSSION

The present comparative model study was motivated by experimental results and their suggested explanations that nonsteroidal anti-inflammatory drugs triggering gastric toxicity interact with lipids that form a protective hydrophobic barrier of gastric mucosa in a way that decreases the hydrophobicity of the barrier.<sup>13,16,17</sup> The aim of the study was to examine the effects of selected NSAIDs on the structural parameters of a POPC-Chol bilayer using both X-ray diffraction and MD simulation methods. MD simulations additionally provided detailed information about the location of the drug molecules in the bilayer as well as their basic atomic-level interactions with POPC and Chol; these interactions were suggested to be the main cause of gastric toxicity induced by some NSAIDs. The studied NSAIDs are three widely used drugs with apparently different gastric toxicity: ketoprofen (KET), aspirin (ASP), and piroxicam (PXM). POPC is the key phospholipid of gastric mucus and mucosa,<sup>29–31</sup> and a POPC-Chol bilayer is a relevant model of the phospholipid oligolamellar structures of the gastric mucosa hydrophobic barrier as well as a gastric mucosa cell membrane (cf. Introduction).

The X-ray diffraction experiment validated our computer modeling because it confirmed that under experimental conditions (20–40 °C, atmospheric pressure) the studied bilayer systems are lamellar and at full hydration they are in the fluid

phase (cf. X-ray Diffraction). Both X-ray diffraction measurements and MD simulations revealed that the effects of NSAIDs on the POPC-Chol bilayer structural parameters are moderate. For reasons explained in the Results section, numerical values for the parameters derived experimentally and computationally cannot be directly compared; nevertheless, the effect of the drugs on the parameters monitored by both methods shows the same trend (Table 1). Unfortunately, the results obtained in this part of the study are not discriminating.

MD simulations show that the drugs interact with polar groups of POPC and/or Chol (Table 4) but not extensively and predominantly via H-bonding. PXM does not interact with POPC, whereas ASP and KET do interact and to a similar extent but only in the neutral states. In general, NSAID $\cdots$ Chol H-bonds are less numerous than NSAID $\cdots$ POPC H-bonds and take place only with ionic and zwitterionic NSAIDs. ASP makes over four times more H-bonds with Chol than do KET and PXM (Table 4), and their number is around 2 times smaller than that with POPC. However, in the bilayer there are  $\sim$ 3.5 times fewer Chol than POPC molecules. This, as well as a relatively long lifetime of ASP $\cdots$ Chol H-bonds (Table 4), might indicate that ASP preferentially interacts with Chol; in contrast, KET makes over 10 times fewer H-bonds with Chol than with POPC. However, it is important to note here that the errors in the numbers of NSAID-POPC and NSAID-Chol H-bonds and their lifetimes are large (cf. NSAID-POPC Hydrogen Bonds).

All drug molecules greatly interact with water by H-bonding, but those in the anionic form make over 3 times more H-bonds with water than do the neutral ones and around 2 times more than the zwitterionic ones (Table 2). Such widespread H-bonding between NSAIDs and water did not seem to be very likely because in all bilayer systems within 30 ns the drug molecules were located in the bilayer interfacial area, mainly on the hydrophobic core side, and remained in this location for the following 30 ns (Figures 5 and S2, Supporting Information). Nevertheless, such an interaction takes place, and anionic KET, which is located deeper in the hydrophobic bilayer core (Figure 6b) makes  $\sim$ 1.5 times more H-bonds with water than does anionic ASP and  $\sim$ 2.5 times more than does zwitterionic PXM, which are less deeply located (Figure 6b).

A reverse relationship to that for water applies to Na $^+$ . Anionic ASP interacts with Na $^+$  2 times more extensively than does anionic KET and 4 times more extensively than does PXM (Figure S4, Supporting Information). At the same time, neutral ASP does not interact with Na $^+$ , whereas neutral KET does very little (Figure 13a). The data in Table 3 indicate that there is no competition between NSAIDs and POPC with respect to interacting with water and Na $^+$ ; NSAIDs practically do not affect the binding of water and Na $^+$  by POPC. Thus, the binding of water and Na $^+$  by NSAID molecules is not at the expense of POPC.

The picture emerging from this MD simulation study is as follows: anionic NSAIDs interact with cholesterol, water, and ions more readily than do zwitterionic and neutral NSAIDs. An exception is NSAID $\cdots$ POPC H-bonding, which can take place only when ASP and KET are H-bond donors, that is, when they are in the neutral form. ASP and KET make comparable numbers of H-bonds with POPC. The location of anionic ASP molecules in the bilayer is shallow (Figures 5 and 6), and they interact both with Chol and Na $^+$ . At the same time, anionic KET molecules that are located more deeply in the interface interact with Chol and Na $^+$  significantly more weakly than does ASP but make nearly 1.5 times more H-bonds with water. This is a large difference because the

average number of H-bonds with water per KET is 4.6 and that for per ASP is 3.3. These numbers significantly exceed the numbers of NSAID $\cdots$ Chol and NSAID $\cdots$ POPC H-bonds per NSAID. Neutral KET and ASP make similar numbers of H-bonds with water but significantly fewer than the anionic ones.

Because anionic KET molecules are located in the bilayer relatively deeply and make a considerable number of H-bonds with water molecules, these water molecules penetrate the bilayer to a greater depth than in the absence of anionic KET. The distribution of the neutral KET molecules in the bilayer is similar to that of the anionic ones, so even though they bind fewer water molecules, they strengthen the effect of deeper water penetration in the bilayer. An example of the bilayer core penetration by two arbitrarily chosen water molecules that are H-bonded to KET in the POPC-KET bilayer is illustrated in Figure S6 (Supporting Information). The neutral ASP molecules are located in a similar bilayer region as neutral KET but make  $\sim$ 15% fewer H-bonds with water. The anionic ASP molecules that are located in the bilayer closer to the water phase make  $\sim$ 40% fewer H-bonds with water than does anionic KET. For both reasons, ASP $\cdots$ water H-bonds have a smaller effect on the depth of water penetration in the bilayer than do KET $\cdots$ water H-bonds. Results concerning ASP $\cdots$ water interactions are in accord with newly published results for ASP in both the neutral and anionic states, partitioning into a saturated PC bilayer using the potential of mean force constrained force method.<sup>66</sup>

From the perspective of the experimental hypothesis relating the gastric toxicity of NSAIDs to their effectiveness in reducing the hydrophobicity of the protective barrier of gastric mucosa,<sup>16,17,20</sup> among the three NSAIDs compared in the present study, KET seems to be the most harmful because it binds more water molecules and is located more deeply in the bilayer than the other two NSAIDs (i.e., ASP and PXM). The relationship between the drug toxicity and its effect on the hydrophobicity of the protective barrier might simply arise from just deeper bilayer penetration by water, which certainly decreases the hydrophobicity of the bilayer core. However, this deeper water might significantly destabilize the bilayer structure and over a longer time may lead to the formation of pores: the water molecules H-bonded to anionic KET might attract lipid headgroups, which results in the deformation of the bilayer surface. Likewise, the binding of Na $^+$  by ASP might affect the bilayer surface, leading to changes in the mechanical properties of the bilayer, as suggested in thoroughly reviewed biophysical studies<sup>21</sup> as well as in the study relating interfacial electrostatic and mechanical properties of the bilayer.<sup>67</sup> Distinguishing which of the interactions is more harmful to the bilayer stability requires further analysis.

## ASSOCIATED CONTENT

**S Supporting Information.** Table with parameters characterizing equilibrated bilayers. Figures showing the equilibration process, density distributions of molecules, atoms and ions in the bilayers, and the interactions of ions with atoms of drugs and phospholipid molecules. This material is available free of charge via the Internet at <http://pubs.acs.org>.

## AUTHOR INFORMATION

### Corresponding Author

\*Tel: +48-12-664-6518. Fax: +48-12-664-6902. E-mail: marta.paseniewicz-gierula@uj.edu.pl

## ■ ACKNOWLEDGMENT

This work was supported by the Ministry of Science and Higher Education of Poland (PB-4553/P01). We are grateful to Prof. Paweł Balgavy for his substantial help and advice and also Drs. Paweł Serda and Tadeusz Librowski for their help in carrying out X-ray diffraction measurements. We thank HASYLAB at DESY, Hamburg, Germany, for beam time and support (Hasylab project I-05-089EC).

## ■ REFERENCES

- (1) Carson, J. L.; Strom, B. L.; Boore, M. L. *Arch. Intern. Med.* **1987**, *147*, 1054–1059.
- (2) Langman, M. J. S.; Weil, J.; Wamright, P. *Lancet* **1994**, *343*, 1075–1078.
- (3) Fries, J. F.; Miller, S. R.; Spitz, P. W.; Williams, C. A.; Hubert, H. B.; Bloch, D. A. *Gastroenterology* **1989**, *96*, 647–655.
- (4) Barrier, C. H.; Hirschowitz, B. I. *Arthritis Rheuma* **1989**, *32*, 926–932.
- (5) Gabriel, S. E.; Jaakkimainen, L.; Bombardier, C. *Ann. Intern. Med.* **1991**, *115*, 787–796.
- (6) Kurata, J. H.; Abbey, D. E. *J. Clin. Gastroenterol.* **1990**, *12*, 260–266.
- (7) Rachmilewitz, D.; Ligumski, M.; Fich, A. *Gastroenterology* **1986**, *90*, 963–969.
- (8) Pollison, R. *Am. J. Med.* **1996**, *100* (Suppl 2A), 31S–36S.
- (9) Vane, J. R.; Botting, R. M. *Scand. J. Rheumatol., Suppl.* **1996**, *102*, 9–21.
- (10) Miller, T. A. *Am. J. Physiol.* **1983**, *245*, G601–G623.
- (11) Wallace, J. L. *Physiol. Rev.* **2008**, *88*, 1547–1565.
- (12) Giraud, M.; Motta, C.; Romero, J. J.; Bommelaer, G.; Lichtenberger, L. M. *Biochem. Pharmacol.* **1999**, *57*, 247–254.
- (13) Lichtenberger, L. M. *Annu. Rev. Physiol.* **1995**, *57*, 565–583.
- (14) Darling, R. L.; Romero, J. J.; Dial, E. J.; Akunda, J. K.; Langenbach, R.; Lichtenberger, L. M. *Gastroenterology* **2004**, *127*, 94–104.
- (15) Davenport, H. W. *Am. J. Dig. Dis.* **1976**, *21*, 141–143.
- (16) Hills, B. A. *Gut* **1996**, *39*, 621–624.
- (17) Lichtenberger, L. M. *Biochem. Pharmacol.* **2001**, *61*, 631–637.
- (18) Spychal, R. T.; Marrero, J. M.; Saverymuttu, S. H.; Northfield, T. C. *Gastroenterology* **1989**, *97*, 104–111.
- (19) Park, J. H.; Robinson, J. R. *Pharm. Res.* **2008**, *25*, 16–24.
- (20) Lichtenberger, L. M.; Barron, M.; Marathi, U. *Drugs Today* **2009**, *45*, 877–890.
- (21) Lichtenberger, L. M.; Zhou, Y.; Dial, E. J.; Raphael, R. M. J. *Pharm. Pharmacol.* **2006**, *58*, 1421–1428.
- (22) Hwang, S.-B.; Shen, T. Y. *J. Med. Chem.* **1981**, *24*, 1202–1211.
- (23) Fan, S. S.; Shen, T. Y. *J. Med. Chem.* **1981**, *24*, 1197–1202.
- (24) Lucio, M.; Bringezu, F.; Reis, S.; Lima, J. L. F. C.; Brezesinski, G. *Langmuir* **2008**, *24*, 4132–4139.
- (25) García-Rodríguez, L. A. *Am. J. Med.* **1998**, *104* (Suppl 3A), 30S–34S.
- (26) McCarthy, D. M. *Am. J. Med.* **1999**, *107* (Suppl 6A), 37S–46S.
- (27) Richy, F.; Bruyere, O.; Ethgen, O.; Rabenda, V.; Bouvenot, G.; Audran, M.; Herrero-Beaufmont, G.; Moore, A.; Eliakim, R.; Haim, M.; Reginster, J.-Y. *Ann. Rheum. Dis.* **2004**, *63*, 759–766.
- (28) Librowski, T.; Czarnecki, R.; Czekaj, T.; Marona, H. *Medicina (Kaunas)* **2005**, *41*, 54–58.
- (29) Bernhard, W.; Postle, A. D.; Linck, M.; Sewing, K. F. *Biochim. Biophys. Acta* **1995**, *1255*, 99–104.
- (30) Ehehalt, R.; Wagenblast, J.; Erben, G.; Lehmann, W. D.; Hinz, U.; Merle, U.; Stremmel, W. *Scand. J. Gastroenterol.* **2004**, *39*, 737–742.
- (31) Ehehalt, R.; Braun, A.; Karner, M.; Füllekrug, J.; Stremmel, W. *Biochim. Biophys. Acta* **2010**, *1801*, 983–993.
- (32) Akaydin, M.; Öğünç, G.; Öner, G. *J. Islamic Acad. Sci.* **1991**, *4*, 257–259.
- (33) Furlan, L.; Catala, A. *Comp. Biochem. Physiol.* **1996**, *113A*, 275–278.
- (34) Dietschy, J. M.; Gamel, W. G. *J. Clin. Invest.* **1971**, *50*, 872–880.
- (35) Wunder, C.; Churin, Y.; Winau, F.; Warnecke, D.; Vieth, M.; Lindner, B.; Zähringer, U.; Mollenkopf, H.-J.; Heinz, E.; Meyer, T. F. *Nat. Med.* **2006**, *12*, 1030–1038.
- (36) Widomska, J.; Raguz, M.; Dillon, J.; Gaillard, E. R.; Subczynski, W. K. *Biochim. Biophys. Acta* **2007**, *1768*, 1454–1465.
- (37) Karlovská, J.; Lohner, K.; Degovics, G.; Lacko, I.; Devinsky, F.; Balgavy, P. *Chem. Phys. Lipids* **2004**, *129*, 31–41.
- (38) Luzzati, V. In *Biological Membranes*, Chapman, D., Ed.; Academic Press: London, 1968; Vol. 1.
- (39) Greenwood, A. I.; Tristram-Nagle, S.; Nagle, J. F. *Chem. Phys. Lipids* **2006**, *143*, 1–10.
- (40) Kucerka, N.; Tristram-Nagle, S.; Nagle, J. F. *J. Membr. Biol.* **2005**, *208*, 193–202.
- (41) Scherer, J. R. *Proc. Natl. Acad. Sci. U.S.A.* **1987**, *84*, 7938–7942.
- (42) Vo, L.; Simonian, H. P.; Doma, S.; Fisher, R. S.; Parkman, H. P. *Aliment. Pharmacol. Ther.* **2005**, *21*, 1321–1330.
- (43) Fieser, L. F.; Fieser, M. *Organic Chemistry*, 3rd ed.; Reinhold Publishing Corporation: New York, 1956.
- (44) Kerns, E. H.; Di, L. *Drug-like Properties: Concepts, Structure, Design, and Methods*; Elsevier: London, 2008.
- (45) Hansch, C. *Comprehensive Medicinal Chemistry*; Pergamon Press: Oxford, U.K., 1990; Vol. 6.
- (46) Gwaka, H.-S.; Choib, J.-S.; Choib, H.-K. *Int. J. Pharmacol.* **2005**, *297*, 156–161.
- (47) www.accelrys.com.
- (48) Mayo, S.; Olafson, B. W. G., III. *J. Phys. Chem.* **1990**, *94*, 8897–8909.
- (49) Gasteiger, J.; Marsili, M. *Tetrahedron* **1980**, *36*, 3219–3228.
- (50) Bockmann, R. A.; Hac, A.; Heimborg, T.; Grubmüller, H. *Biophys. J.* **2003**, *85*, 1647–1655.
- (51) Jorgensen, W. L.; Tirado-Rives, J. *J. Am. Chem. Soc.* **1988**, *110*, 1657–1666.
- (52) Jorgensen, W. L.; Chandrasekhar, J.; Madura, J. D.; Impey, R.; Klein, M. L. *J. Chem. Phys.* **1983**, *79*, 926–935.
- (53) Cornell, W. D.; Cieplak, P.; Bayly, C. I.; Kollman, P. A. *J. Am. Chem. Soc.* **1993**, *115*, 9620–9631.
- (54) www.gaussian.com.
- (55) Essmann, U.; Perera, L.; Berkowitz, M. L.; Darden, T.; Lee, H.; Pedersen, L. G. *J. Chem. Phys.* **1995**, *103*, 8577–8593.
- (56) Seelig, J.; Waespe-Sarcevic, N. *Biochemistry* **1978**, *17*, 3310–3315.
- (57) Berendsen, H. J. C.; Postma, J. P. M.; van Gunsteren, W. F.; DiNola, A.; Haak, J. R. *J. Chem. Phys.* **1984**, *81*, 3684–3690.
- (58) Hyslop, P. A.; Morel, B.; Sauerheber, R. D. *Biochemistry* **1990**, *29*, 1025–1038.
- (59) Brzozowska, I.; Figaszewski, Z. A. *Colloids Surf., B* **2002**, *23*, 51–58.
- (60) Smaby, J. M.; Momsen, M.; Brockman, H. L.; Brown, R. E. *Biophys. J.* **1997**, *73*, 1492–1505.
- (61) Shieh, H.-S.; Hoard, L. G.; Nordman, C. E. *Acta Crystallogr. 1981*, *B37*, 1538–1543.
- (62) Nagle, J. F.; Tristram-Nagle, S. *Biochim. Biophys. Acta* **2000**, *1469*, 159–195.
- (63) Rappolt, M. *J. Appl. Phys.* **2010**, *107*, 084701–1–7.
- (64) Hubbell, W. L.; McConnell, H. M. *J. Am. Chem. Soc.* **1971**, *93*, 314–326.
- (65) Luzar, A. *J. Chem. Phys.* **2000**, *113*, 10663–10675.
- (66) Boggara, M. B.; Krishnamoorti, R. *Biophys. J.* **2010**, *98*, 586–595.
- (67) Zhou, Y.; Raphael, R. M. *Biophys. J.* **2007**, *92*, 2451–2462.
- (68) Rog, T.; Pasenkiewicz-Gierula, M. *Biochimie* **2006**, *88*, 449–460.